

Chronology of coastal dune ridges in Vaigai prodelta region, southeastern Tamil Nadu, India

S. Sathiyaseelan¹, D. K. Panda², D. Banerjee^{2,*}, D. Ramesh¹ and A. D. Shukla²

¹Department of Remote Sensing, Bharathidasan University, Tiruchirappalli 620 023, India

²Physical Research Laboratory, Ahmedabad 380 009, India

The Tamil Nadu coastline, India, has extensive dunes which can be used for inferring quaternary palaeoclimates. In the present study, we aim to determine the chronology of the dunes in the Vaigai prodelta region along the southeastern coastline of the country. Optically stimulated luminescence ages for the elevated beach ridge samples SANK-5, SANK-4, SANK-3, SANK-2 and SANK-1 were estimated to be 0.9 ± 0.1 , 1.1 ± 0.1 , 1.8 ± 0.2 , 5.3 ± 0.4 and 27 ± 2.3 ka respectively, from top to bottom of the section. The first four phases of aeolian activation occurred in marine oxygen isotope stage-1, whereas the ~ 27 ka age suggests that sediment deposition occurred in marine oxygen isotope stage-3. The luminescence ages were in stratigraphic order, and represent the first dates of aeolian activation in the Vaigai region.

Keywords: Aeolian activation, chronology, coastline, luminescence ages, palaeoclimate, red dunes.

THE Quaternary period is of great interest to geoscientists for inferring the ecological, environmental and climatic changes. Although several global studies have been carried out on coastal dunes, the southern part of the Indian peninsula has not been largely examined in respect of geochronology. It has been previously suggested that geometry, orientation and elevation of beach-ridge sets and plains are good indicators of past sea levels, morphodynamic and climatic conditions. The Tamil Nadu coastline, India, has extensive dunes which can be used for inferring quaternary paleoclimates. Teri sands, i.e. weathered red dunes occur inland, whereas white dunes are prevalent along the present shoreline. Dune reddening has been previously suggested to be post-depositional^{1,2}, and due to *in situ* weathering of feldspar grains¹. Earlier chronological studies have suggested that near-coastal dunes aggraded at ~ 5.6 ka, and coastal Teri dune deposition occurred before ~ 11.4 ka (ref. 2). The present study aims to determine the chronology of dunes in the Vaigai prodelta region in Tamil Nadu, along the southeastern coastline of India.

The study area is located in the Vaigai delta which lies within $9^{\circ}14' - 9^{\circ}30'N$ lat and $77^{\circ}48' - 79^{\circ}11'E$ long (Figure 1). Generally, the study area experiences hot tropical climate with temperature ranging from $22^{\circ}C$ to $38^{\circ}C$. The annual average rainfall is 750–830 mm, with $\sim 60\%$ it received during the northeast monsoon months (September to November), whereas the southwest monsoon months (June to August) contributes around 25%. The sampling site is located ~ 8 km from the present-day coastline.

The Vaigai is a major river originating in the Western Ghats and flows eastwards with a prominent arcuate delta in the chosen study area. Geologically, the study area is covered by Quaternary marine sediments. Geomorphically, the study area has many different landforms such as deltaic plain, palaeochannels, beaches, beach ridges, emerged beach rocks, dunes, swales, tidal flats and Teri/red sediments deposited during the Quaternary. The palaeochannel deposits comprise of brown-coloured, fine to medium sands with well-preserved cross-beddings. The fluvio-marine and marine deposits are well exposed in the prodelta region of Vaigai river. The Vaigai prodelta has a pattern of beach ridges with six ridges oriented in a southerly direction (NE–SW), whereas two beach ridges are oriented (NW–SE) in the northern part of the study area. Sanganthiyanvalasai is the sampling site ($78^{\circ}53'54.162''E$; $9^{\circ}18'41.387''N$) located in the inner part of the beach ridge complex, and is about 11 m amsl. A trench was made at the sampling location up to 3.5 m depth. The exposed trench has three different stratigraphic layers of different thickness. Figures 1 and 2 show the different lithologies of the trench. The uppermost layer has loose unconsolidated fine sand and is underlain by a highly silty, medium sand layer. The bottom layer primarily comprises of coarse, calcareous sand deposits.

Experimental details

Samples were collected in opaque tubes by driving the tubes horizontally into the stratigraphic section or collected as sand blocks from the indurated section, and sealed immediately using light, tight, black plastic bags in the field. The light-exposed outer parts of the block

*For correspondence. (e-mail: deba@prl.res.in)

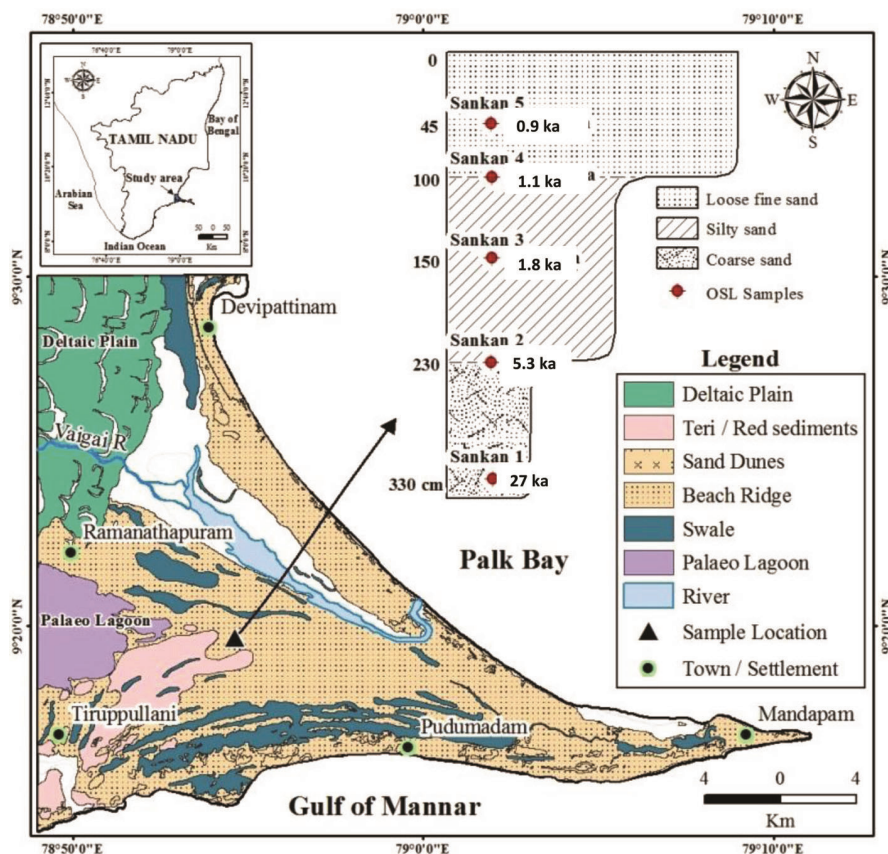


Figure 1. Location of sampling sites in Tamil Nadu, India.

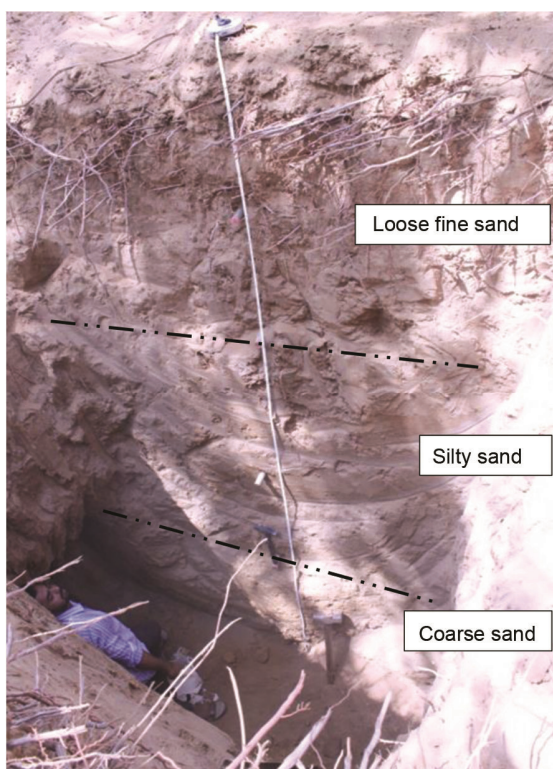


Figure 2. Lithology of trench site at Sanganthiyanvalasai, Tamil Nadu.

samples were removed in the laboratory under red light and the unexposed inner parts were used for optically stimulated luminescence (OSL) dating. Samples were dry-sieved under subdued red light and the sand fraction of 90–150 μm grain size was used for further treatment. This included dissolution using 1 N hydrochloric acid (HCl), and removal of organic matter with 30% hydrogen peroxide (H_2O_2). Quartz grains were obtained after etching samples with 40% hydrofluoric acid (HF) for 1 h. An automated Riso TL/OSL DA-15 reader attached to a $^{90}\text{Sr}/^{90}\text{Y}$ beta source was used for luminescence measurements. OSL signals were detected using U-340 filters, whereas infrared and post-infrared stimulated (pIRIR) signals were detected using a combination of Corning 7-59 and Schott BG39 filters.

Figure 3 shows the thermoluminescence (TL) signal in the 0°–200°C temperature region from a 1.2 Gy regeneration dose for all five samples. It is noteworthy that in every sample, the low-temperature (~110°C) TL peak characteristic of quartz mineralogy is apparent. However, TL counts in the 160°–200°C temperature region are not similar for all five samples. SANK-1 has negligible TL counts in this region (integral counts ~5300), while SANK-2 has an order of magnitude higher TL signal level (integral counts ~52,000) in the same region. Other samples (SANK-3, SANK-4 and SANK-5) have intermediate

TL signal levels, with integral TL counts ranging from 13,000 to 20,000. Further, post-IRIR signals were observed despite etching all five samples in 40% HF for 1 h. This is not surprising; Huntley *et al.*³ have previously dated stranded beach dunes in South Australia using IR-stimulated signals from micron-sized K-feldspar inclusions within quartz grains. In light of these observations, the present study determined luminescence ages using the single-aliquot regenerative-dose (SAR) procedure^{4,5} for OSL, and IR and post-IRIR ages using a modified SAR protocol as described in the literature^{6,7}.

OSL measurements on all samples involved preheating (heating prior to measurement of natural or laboratory-irradiated signals) natural and regenerated signals at 260°C. Dose rate measurements were carried out on dried samples, which were packed and sealed air-tight to prevent radon loss. The samples were stored for one month after sealing to re-establish ²²⁶Ra–²²²Rn equilibrium. External dose rate estimation (Table 1) required measurement of activity of ²³⁸U (²¹⁴Bi and ²¹⁴Pb), ²³²Th (²²⁸Ac, ²¹²Pb and ²⁰⁸Tl) and 40 K from high-resolution gamma spectrometry (high purity germanium detector, HPGe; Table 1). The water content was assumed to be ~10% for all samples throughout the burial period. The α -value was assumed to be ~0.05 in alpha dose-rate estimation for infrared stimulated luminescence (IRSL) and post-IRIR age determination, whereas the internal K-content was presumed to be ~13% in dose-rate calculations. The alpha

dose-rate contribution was ~10% of the total dose-rate estimate used in IRSL and post-IRIR age determination for the samples.

Luminescence characteristics

A principal assumption in the determination of equivalent dose is that luminescence signals are stable over geological timescales. We have checked the thermal stability of post-IR regenerated IRSL signals for sample SANK-5. The measured post-IR IRSL signals were normalized with respect to their initial values (Figure 4 *a*). As expected, the regenerative first-IR pulse sensitivity corrected pulse-anneal curves showed significant loss of IRSL signal due to thermal erosion at temperatures beyond 275°C. Zhang *et al.*⁸ observed the first-IR pulse sensitivity-corrected signals to decrease continuously from preheat temperatures beyond 200°C and reduce to 10% of their initial value at temperatures of ~300°C. In contrast, the sensitivity-corrected post-IRIR signal decreased to 80% of its initial value at 300°C for SANK-5, as observed previously. These observations suggest a higher thermal stability of the pIRIR signal with respect to the IRSL signal, as previously reported by Li and Li⁹ for K-rich feldspar extracts. Next, we tested the thermal stability of the OSL signal for sample SANK-1. An aliquot was stimulated

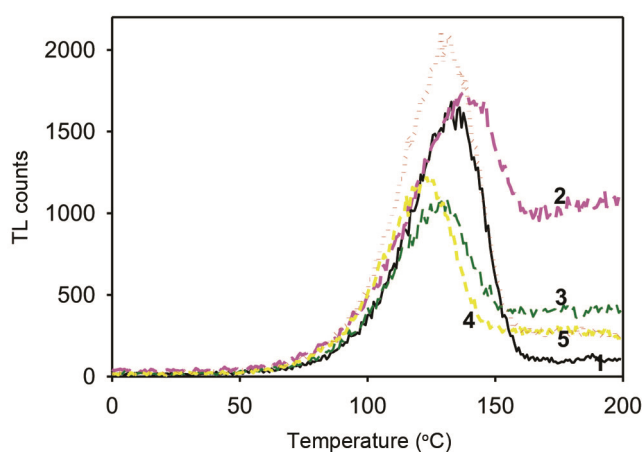


Figure 3. Thermoluminescence signals from SANKAN samples measured after 1.2 Gy beta irradiation.

Table 1. Radionuclide concentrations for SANKAN samples

Sample	Potassium (%)	Thorium (ppm)	Uranium (ppm)
SANK-5	1.26	4.0	0.7
SANK-4	1.53	4.2	0.9
SANK-3	1.57	7.0	0.9
SANK-2	1.72	8.3	1.2
SANK-1	1.7	9.4	1.1

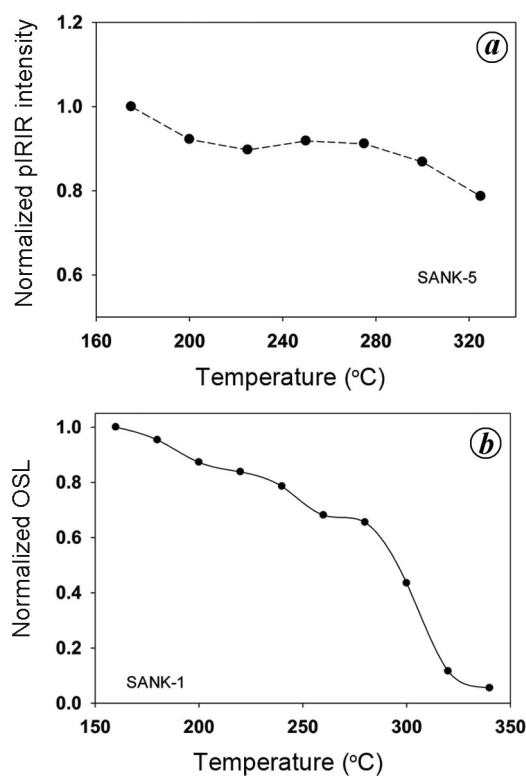


Figure 4. *a*, Variation of pIRIR signal with preheat temperature (pulse annealing curve) for sample SANK-5. *b*, Variation of optically simulated signal with preheat temperature for sample SANK-1.

at 280°C for 100 s for resetting, and then given a regeneration dose of 480 Gy. It was then heated to 160°C for 10 s before 0.1 s OSL measurement at 125°C and with low stimulation power (0.5% of maximum). This sequence was repeated with the preheat temperature being increased in 20°C steps up to 340°C, each followed by 0.1 s OSL measurements at 125°C. Figure 4b shows the regenerative signals normalized with respect to the initial value (OSL observed after 10 s, 160°C preheat). The OSL signal exhibits fast decay between 260°C and 320°C, consistent with the main trap being identified as the 325°C TL trap¹⁰, a characteristic typically associated with quartz OSL.

In the pIRIR measurements, the same preheat conditions were used before measurement of the natural, regenerative and test doses. The first IR stimulation was carried out at 60°C for 200 s, followed by the second stimulation at 290°C as discussed in Buylaert *et al.*⁷. We also used a pretest dose thermal wash of 260°C for 100 s as suggested by Lamothe *et al.*¹¹ for improving dose-recovery ratio (DRR) in the pIRIR SAR procedure. The D_e (equivalent dose) values were estimated using signals integrated over the first 4 s, while background estimation was done from the last 20 s. If one presumes that thermally assisted tunnelling uses up increasingly distant electron-hole pairs, it is expected that increasing the first IR stimulation temperature might result in a more stable pIRIR signal. Following the post-IRIR procedure outlined in Buylaert *et al.*⁷, we have studied the dependence of equivalent dose on prior-IR stimulation temperature using a preheat temperature of 275°C for 60 s. Figure 5 shows a plot of equivalent dose for SANK-3 as a function of prior-IR stimulation temperature. The average equivalent dose was estimated to be $\sim 23 \pm 0.8$ Gy, and agrees (at 2σ level) with the D_e values determined for various prior-IR stimulation temperatures ranging from 60°C to 210°C. Thus, there is little evidence that varying the first IR stimulation temperature has any significant effect on equivalent dose estimation. Based on this plateau, any of the above prior-IR stimulation temperatures can be chosen; however, the subsequent post-IRIR signal is significantly

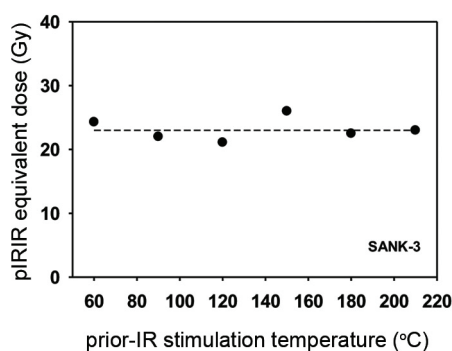


Figure 5. Dependence of equivalent dose on prior-IR stimulation temperature for SANK-3.

reduced as the first-IR stimulation temperature is increased beyond 60°C. Hence, it is desirable to choose a low IR stimulation temperature in the post-IRIR procedure for equivalent dose determination.

Results

Figure 6 shows typical OSL and pIRIR₂₉₀ growth curves for samples SANK-5 and SANK-2 respectively. In Figure 7, the mean equivalent dose for the pIRIR signals is plotted against preheat temperature for sample SANK-5. A D_e plateau is observed between 220°C and 320°C preheat temperature for SANK-5, with average equivalent dose estimated to be 3.3 ± 0.3 Gy. For polymineral 4–11 μ m grains, Zhang *et al.*⁸ observed a D_e plateau between 240°C and 280°C, whereas others have reported the plateau at temperatures in excess of 250°C. Dose-recovery tests carried out using SAR procedure for OSL indicated DRR of 0.98 ± 0.02 for sample SANK-1.

Previous studies have shown that the resetting of pIRIR₂₉₀ signal by sunlight is less effective than that for IRSL signals^{12,13}, and thus greater residual signals may be expected in pIRIR signals in comparison to IRSL. In Figure 8, the pIRIR₂₉₀ equivalent dose estimates are plotted

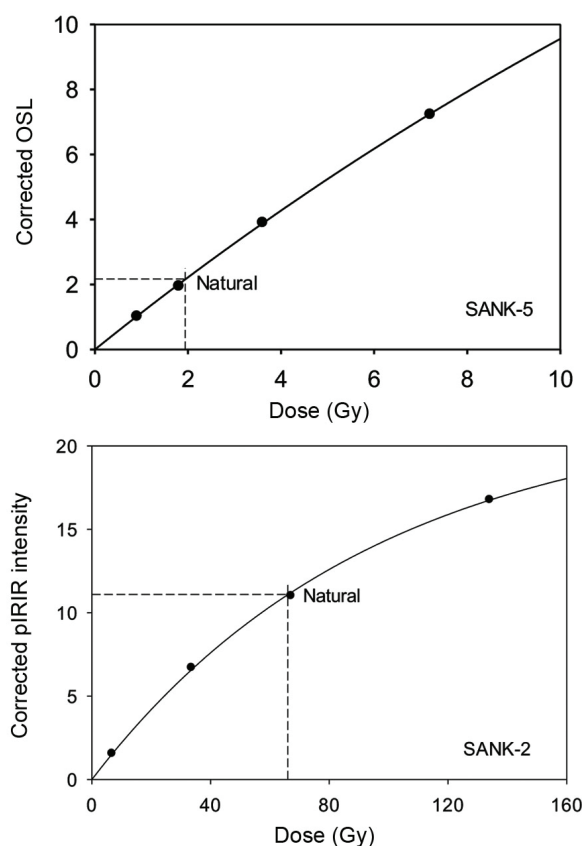


Figure 6. Sensitivity-corrected OSL and pIRIR₂₉₀ intensity plotted as a function of regeneration dose (growth curve) for SANK-5 and SANK-2 respectively.

against the IR_{60} equivalent dose and exhibit a strong linear correlation ($r^2 = 0.98$). An interpretation of the data is that the total IRSL signal is made up of two components, one related to a trap which can be emptied by IR stimulation at 60°C , whereas the other trap can only be emptied by IR stimulation at elevated temperatures. However, another explanation may be related to the observation that IR_{60} signals are significantly affected by anomalous fading resulting in D_e underestimation, whereas $pIRIR_{290}$ signals exhibit much smaller fading rates⁷. Furthermore, we consider that both $pIRIR_{290}$ and IR_{60} signals have not been completely reset at deposition, particularly for samples SANK-2, SANK-3 and SANK-4 (Table 2). OSL and IR_{60} ages for SANK-5 agree with each other, and the corresponding ages for SANK-1 are consistent if 2σ error limits are considered. Godfrey-Smith *et al.*¹⁴ have shown that the quartz OSL signal resets faster than the IRSL signal. Murray *et al.*¹⁵ have

demonstrated that resetting of the IRSL signal is faster than that of the $pIRIR_{290}$ signal. Hence, the discussion below relates to OSL ages obtained in this study.

Implications of luminescence ages

The quartz OSL ages for elevated coastal sand dune ridge samples SANK-5, SANK-4, SANK-3, SANK-2 and SANK-1 are 0.9 ± 0.1 , 1.1 ± 0.1 , 1.8 ± 0.2 , 5.3 ± 0.4 and 27 ± 2.3 ka respectively (Tables 2 and 3), from top to bottom of the section. The ages suggest that these sediments were deposited between marine isotope stages 1 and 3 (ref. 16). These ages are in stratigraphic order and represent the first dates of aeolian activation in the Vaigai region. The younger parts of the beach ridges are often influenced by human activities in the study area. Table 2 present the equivalent dose, dose-rate and luminescence ages of the samples.

While the present study suggests that the upper layer of sediments with thickness of ~ 2.5 m was deposited during the Holocene, Alappat *et al.*¹⁷, have reported that deposition of the upper 5 m layer from the surface of the Cauvery deltaic sediments took place during the Holocene. This is likely because the Vaigai delta is not mature like the Cauvery; hence the sedimentation rate is much lower. Further, active tectonics may have initiated erosional activity in the southern part of the Vaigai region. Alappat *et al.*¹⁸ have determined ages of red dune sands in the southwest coast of Tamil Nadu. Their OSL ages suggested two events of deposition with sands in the upper part being deposited during 16–13 ka, whereas the indurated layer in terrace 2 was deposited at 4.5 ka. Previous studies have shown that monsoon precipitation intensified in the region as early as 14 ka and was dominant until up to 7 ka (ref. 19). It has been suggested that monsoon intensification during the Holocene occurred at ~ 11 , ~ 9 –6 and ~ 1.5 –2 ka (ref. 20).

It is significant that periods of monsoon intensification during the late Holocene (~ 6 and ~ 1 –2 ka) are coincidental with periods of aeolian activity in the Vaigai region. Furthermore, during the early Holocene, we speculate that dune-building activity may have stopped due to reduced sand supply in the region. Aggradation is more prevalent during lower sea-level stands, when part of the continental shelf was exposed providing available sand for aeolian reworking and is perhaps related to large-scale aggradations during last glacial maximum (LGM) in the river sequences along the west coast of India²¹. Studies on sea-level changes in the east and west coasts suggest that between 7 and 3 ka the sea level was ~ 3 m higher than the present level, with a brief lowering from the earlier position at 5 ka (ref. 22). The higher sea level is likely to have deposited large volumes of sand at the lower terrace as beach deposits. This stage is represented by a number of coast-parallel beach ridges, both in the east

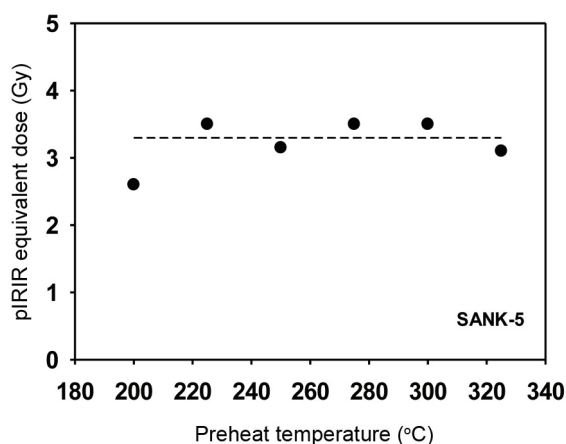


Figure 7. Dependence of $pIRIR_{290}$ equivalent dose on preheat temperature for SANK-5.

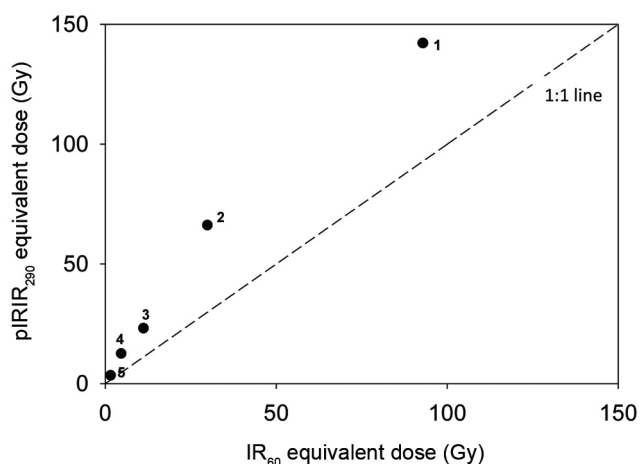


Figure 8. $pIRIR_{290}$ equivalent dose plotted against IR_{60} equivalent dose for SANKAN samples.

Table 2. Dose rate, equivalent dose and age estimate for SANKAN samples

Sample	Depth (m)	OSL equivalent dose (Gy)	Dose-rate (mGy/a)	OSL ages (ka)
SANK-1	3.3	75 ± 6	2.78 ± 0.15	27 ± 2.3
SANK-2	2.3	14.6 ± 1.0	2.77 ± 0.14	5.3 ± 0.4
SANK-3	1.5	4.5 ± 0.4	2.49 ± 0.12	1.8 ± 0.2
SANK-4	1.0	2.6 ± 0.3	2.28 ± 0.11	1.1 ± 0.1
SANK-5	0.45	1.84 ± 0.2	2.0 ± 0.10	0.92 ± 0.1

Table 3. IRSL and pIRIR equivalent dose and age estimates for SANKAN samples

Sample	Depth (m)	Equivalent dose (Gy)		Dose rate (mGy/a)*	Ages (ka)	
		IR ₆₀	pIRIR ₂₉₀		IR ₆₀	pIRIR ₂₉₀
SANK-1	3.3	93 ± 9	142 ± 10	3.15 ± 0.28	30 ± 2.8	45 ± 4.3
SANK-2	2.3	30 ± 2.8	66 ± 6.5	3.12 ± 0.25	9.6 ± 0.9	21 ± 2.0
SANK-3	1.5	11.3 ± 0.9	23 ± 2.5	2.78 ± 0.15	4.1 ± 0.4	8.3 ± 0.8
SANK-4	1.0	4.8 ± 0.5	12.4 ± 1.3	2.49 ± 0.12	1.9 ± 0.2	5 ± 0.5
SANK-5	0.45	1.7 ± 0.2	3.3 ± 0.3	2.18 ± 0.10	0.8 ± 0.1	1.5 ± 0.2

*Estimated assuming water content of 10% and internal K content of 13% for all samples. Small aliquots (up to 20 per sample), with ≤100 luminescent grains per aliquot were used for luminescence measurements and equivalent dose estimation.

and the west coastlines of South India²³. The OSL age of ~5.3 ka suggests sands were being deposited at 5300 ka, and is consistent with previous findings. This also agrees with the inference that aeolian reworking did not begin in this region until ~6 ka ago. Jayangondaperumal *et al.*² have found that coastal red sand in the east coast of India was deposited before 11 ka in association with lower sea level, and the near-coastal red sand was deposited during the sea-level high stand at 6 ka. Furthermore, aeolian reactivation continued till 2000 years ago, and OSL dates from Alappat *et al.*¹⁸ show sands from the upper part of the dunes in the southwestern coastline were also deposited during the last ~400 years. Singhvi *et al.*²⁴, have determined TL ages of Sri Lankan coastal dunes in Bundala and Patirajavela, and showed that two episodes of aeolian accumulation occurred at ~25 and ~70 ka ago. The SANK-1 age of ~27 ka is similar to the ~25 ka age, and indicates that aeolian activity was prominent in both these regions around that time. Gardner¹ obtained radiocarbon dates from land snails in aeolianite in Indian teris and ages of 25,000 years BP. These ages led to the inference that dune deposition and weathering, to a maximum depth of 10 m, resulted in hematite formation, and has taken place rapidly over the past 25,000 years.

- Gardner, R. A. M., Reddening of dune sands – evidence from southeast India. *Earth Surface Process. Landforms*, 1981, **6**, 459–468.
- Jayangondaperumal, R., Murari, M. K., Sivasubramanian, P., Chandrasekhar, N. and Singhvi, A. K., Luminescence dating of fluvial and coastal red sediments in SE coast, India, and implications for paleoenvironmental changes and dune reddening. *Quaternary Res.*, 2012, **77**, 468–481.

- Huntley, D. J., Hutton, J. T. and Prescott, J. R., Optical dating using inclusions within quartz grains. *Geology*, 1993, **21**, 1087–1090.
- Banerjee, D., Bøtter-Jensen, L. and Murray, A. S., Retrospective dosimetry: estimation of the dose to quartz using the single-aliquot regenerative-dose protocol. *Appl. Radiat. Isot.*, 2000, **52**, 831–844.
- Murray, A. S. and Wintle, A. G., Luminescence dating of quartz using an improved single-aliquot regenerative-dose protocol. *Radiat. Meas.*, 2000, **32**, 57–73.
- Thiel, C., Buylaert, J. P., Murray, A. S., Terhorst, B., Hofer, I., Tsukamoto, S. and Frechen, M., Luminescence dating of the Stratzing loess profile (Austria) – testing the potential of an elevated temperature post-IR IRSL protocol. *Quaternary Int.*, 2011, **234**, 23–31.
- Buylaert, J. P., Jain, M., Murray, A. S., Thomsen, K. J., Thiel, C. and Sohbaty, R., A robust feldspar luminescence dating method for Middle and Late Pleistocene sediments. *Boreas*, 2012, **41**, 435–451.
- Zhang, J., Tsukamoto, S., Nottebaum, V. and Lehmkuhl, F., *De* plateau and its implications for post-IR IRSL dating of polymineral fine grains. *Quaternary Geochronol.*, 2015, **30**, 147–153.
- Li, B. and Li, S. H., Thermal stability of infrared stimulated luminescence of sedimentary K-feldspar extracts. *Radiat. Meas.*, 2011, **46**, 29–36.
- Banerjee, D., Murray, A. S., Bøtter-Jensen, L. and Lang, A., Equivalent dose estimation using a single aliquot of polymineral fine grains. *Radiat. Meas.*, 2001, **33**, 73–94.
- Lamothe, M., Forget Brisson, L. and Hardy, F., Dose recovery performance in double IRSL/pIRIR SAR protocols. *Radiat. Meas.*, 2018, **120**, 120–123.
- Colarossi, D., Duller, G. A. T., Roberts, H. M., Exploring the behaviour of luminescence signals from feldspars: implications for the single aliquot regenerative dose protocol. *Radiat. Meas.*, 2018, **109**, 35–44.
- Rashidi, Z., Sohbaty, R., Karimi, A., Farpoor, M. H., Khormali, F., Thomson, W. and Murray, A. S., Constraining the timing of palaeosol development in Iranian arid environments using OSL dating. *Quaternary Geochronol.*, 2019, **49**, 92–100.

RESEARCH ARTICLES

14. Godfrey-Smith, D. I., Huntley, D. J. and Chen, W. H., Optical dating studies of quartz and feldspar sediment extracts. *Quaternary Sci. Rev.*, 1988, **7**, 373–380.
15. Murray, A. S., Thomsen, K. J., Masuda, N., Buylaert, J. P. and Jain, M., Identifying well bleached quartz using the different bleaching rates of quartz and feldspar luminescence signals. *Radiat. Meas.*, 2012, **47**, 688–695.
16. Railsback, L. B., Gibbard, P. L., Head, M. J., Voarintsoa, N. R. G. and Toucanne, S., An optimized scheme of lettered marine isotope substages for the last 1.0 million years, and the climatostratigraphic nature of isotope stages and substages. *Quaternary Sci. Rev.*, 2015, **111**, 94–106.
17. Alappat, L., Frechen, M., Ramesh, R., Tsukamoto, S. and Srinivasalu, S., Evolution of late Holocene coastal dunes in the Cauvery delta region of Tamil Nadu, India. *J. Asian Earth Sci.*, 2011, **42**, 381–397.
18. Alappat, L., Joseph, S., Tsukamoto, S., Kaufhold, S. and Frechen, M., Chronology and weathering history of red dunes in the southwest coast of Tamil Nadu, India. *German J. Geol.*, 2016, **168**, 183–198.
19. Tiwari, M., Singh, A. K. and Ramesh, R., High-resolution monsoon records since the last glacial maximum: a comparison of marine and terrestrial paleoarchives from South Asia. *J. Geophys. Res.*, 2011; doi:10.1155/2011/765248.
20. Overpeck, J., Anderson, D., Trumbore, S. and Prell, W., The southwest Indian monsoon over the last 18,000 years. *Climate Dynamics*, 1996, **12**, 213–225.
21. Kale, V. S. and Rajaguru, S. N., Late Quaternary alluvial history of northwest Deccan Upland region. *Nature*, 1987, **325**, 612–614.
22. Banerjee P. K., Holocene and Late Pleistocene relative sea level fluctuations along the east coast of India. *Mar. Geol.*, 2000, **167**, 243–260.
23. Kunz, A., Frechen, M., Ramesh, R. and Urban, B., Luminescence dating of late Holocene dunes showing remnants of early settlement in Cuddalore and evidence of monsoon activity in south east India. *Quaternary Int.*, 2010, **222**, 194–298.
24. Singhvi, A. K., Deraniyagala, S. U. and Sengupta, D., Thermoluminescence dating of Quaternary red sand beds. A case study of coastal dunes in Sri Lanka. *Earth Planet. Sci. Lett.*, 1986, **80**, 139–144.

ACKNOWLEDGEMENT. D.R. and S.S. thank the Board of Research in Nuclear Sciences, Mumbai and Atomic Mineral Directorate for Exploration and Research, Hyderabad for financial support.

Received 16 September 2020; revised accepted 20 October 2020

doi: 10.18520/cs/v120/i2/382-388
